Verification of New Floating Capabilities in FAST v8

Preprint

F. Wendt, A. Robertson, J. Jonkman,
and G. Hayman
National Renewable Energy Laboratory

NOTICE

This report is available at no cost from the National Renewable Energy Laboratory (NREL) at www.nrel.gov/publications.

Available electronically at http://www.osti.gov/scitech

Available for a processing fee to U.S. Department of Energy and its contractors, in paper, from:

> U.S. Department of Energy
> Office of Scientific and Technical Information
> P.O. Box 62
> Oak Ridge, TN 37831-0062
> phone: 865.576.8401
> fax: 865.576.5728
> email: mailto:reports@adonis.osti.gov

Available for sale to the public, in paper, from:

> U.S. Department of Commerce
> National Technical Information Service
> 5285 Port Royal Road
> Springfield, VA 22161
> phone: 800.553.6847
> fax: 703.605.6900
> email: orders@ntis.fedworld.gov
> online ordering: http://www.ntis.gov/help/ordermethods.aspx

Verification of New Floating Capabilities in FAST v8

Fabian Wendt[1], Amy Robertson[2], Jason Jonkman[3], and Greg Hayman[4]
National Renewable Energy Laboratory, Golden, CO, 80401

FAST v8 is the latest release of the National Renewable Energy Laboratory's wind turbine aero-hydro-servo-elastic simulation software, with several new capabilities and major changes from the previous version. FAST has been significantly altered to improve the simulator's modularity and to include new functionalities in the form of modules in the FAST v8 framework. This paper focuses on the improvements made for the modeling of floating offshore wind systems. The most significant change was to the hydrodynamic load calculation algorithms, which are embedded in the HydroDyn module. HydroDyn is now capable of applying strip-theory (via an extension of Morison's equation) at the member level for user-defined geometries. Users may now use a strip-theory-only approach for applying the hydrodynamic loads, as well as the previous potential-flow (radiation/diffraction) approach and a hybrid combination of both methods (radiation/diffraction and the drag component of Morison's equation). Second-order hydrodynamic implementations in both the wave kinematics used by the strip-theory solution and the wave-excitation loads in the potential-flow solution were also added to HydroDyn. The new floating capabilities were verified through a direct code-to-code comparison. We conducted a series of simulations of the International Energy Agency Wind Task 30 Offshore Code Comparison Collaboration Continuation (OC4) floating semisubmersible model and compared the wind turbine response predicted by FAST v8, the corresponding FAST v7 results, and results from other participants in the OC4 project. We found good agreement between FAST v7 and FAST v8 when using the linear radiation/diffraction modeling approach. The strip-theory-based approach inherently differs from the radiation/diffraction approach used in FAST v7 and we identified and characterized the differences. Enabling the second-order effects significantly improved the agreement between FAST v8 and the other OC4 participants.

Nomenclature

$A_{33}(0)$ = zero-frequency limit of added mass in the heave direction (calculated via WAMIT)
C_{Ai} = added-mass coefficient in the heave direction of joint i
L = angular momentum
ρ_w = water density
$\overrightarrow{V_{ni}}$ = weighted normal reference volume vector of joint i
ω = angular velocity

I. Introduction

THE National Renewable Energy Laboratory's (NREL's) aero-hydro-servo-elastic wind turbine simulation software, FAST, is a comprehensive software tool for the simulation of land-based and offshore wind turbines [1]. The latest release (FAST v8) introduced several major modifications and new capabilities. The architecture of FAST v8 is entirely different from FAST v7. FAST is now split into multiple modules coupled with a driver

---

[1]Engineer, National Wind Technology Center, 15013 Denver West Parkway, Golden, CO 80401
[2]Senior Engineer, National Wind Technology Center, 15013 Denver West Parkway, Golden, CO 80401
[3]Senior Engineer, National Wind Technology Center, 15013 Denver West Parkway, Golden, CO 80401, AIAA Professional Member
[4]Senior Engineer, National Wind Technology Center, 15013 Denver West Parkway, Golden, CO 80401

program (glue code) [2]. The increased modularity aims towards simplifying and improving the development process of future FAST modules developed by NREL and the global user/developer community. Because of the significant program changes in FAST v8, we conducted a series of studies to verify the results generated by FAST v8 against those from FAST v7 and against the corresponding simulation results of other Offshore Code Comparison Collaboration Continuation (OC4) participants. The verification work covered in this paper focuses on the new features introduced to the HydroDyn module, in particular the ballasting feature and the implementation of strip-theory for multimember structures. The new quasi-static mooring line module (MAP) [3], the new second-order hydrodynamics of HydroDyn, and the coupling approach that is used in the modular architecture of FAST v8 are also verified within the scope of this paper. The OC4-DeepCwind semisubmersible was used for the study, and the load cases simulated were those examined in the OC4 Phase II project [4] [5]. The simulated load cases covered a wide range of operating conditions and model complexity. All results in this paper are based on the latest release of FAST, v8.09.00a-bjj.

II. Major Changes Introduced in FAST v8

In FAST v8, major changes have been introduced to the architectural concept of the software. FAST is now divided into individual modules that are executed and coupled with the FAST driver (glue code). A comparison between FAST v7 and FAST v8 architectures is given in Figure 1. Because of its modular architecture, FAST v8 requires a coupling routine that connects different modules. The coupling approach used in FAST v8 features a mesh-to-mesh mapping scheme that allows the coupling of modules with highly different spatial discretization. Data between the modules are exchanged with an implicit predictor-corrector approach, which allows the transfer of platform accelerations from ElastoDyn to HydroDyn and the transfer of hydrodynamic loads, including acceleration-dependent added-mass loads, from HydroDyn to ElastoDyn [6].

Several major changes have been introduced to the HydroDyn module. In FAST v7, HydroDyn calculates the hydrodynamic loads on floating substructures based on a potential-flow theory approach. This approach requires a set of hydrodynamic coefficients (restoring matrix and frequency-dependent damping matrix, added-mass matrix, and wave-excitation vector) that needs to be calculated separately, prior to running FAST. WAMIT [7] is commonly
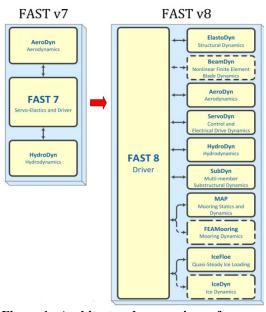

Figure 1. Architectural comparison of FAST v7 and FAST v8 [2].

used to derive these coefficients for a user-specified platform geometry. FAST v7 also calculates the viscous drag on the central substructure member by dividing the member into strips and calculating drag based on the nonlinear viscous-drag term from Morison's equation [8]. Although FAST v8 still offers the potential-flow-theory-based approach for the calculation of wave diffraction and radiation loads, the strip-theory functionality of HydroDyn has been significantly extended. The user can now specify an arbitrary multimember substructure geometry with varying drag, added mass, and dynamic pressure coefficients for each member in FAST's HydroDyn input file. In addition, the other components of the relative form of Morison's equation have been added to the code (fluid-inertia and added-mass terms), enabling the user to model the hydrodynamic loads solely using strip-theory. Other attributes include extensions to Morison's equation, including the ability to model axial hydrodynamic loads on tapered members and member end plates, buoyancy and ballasting of the members, and marine growth. A detailed description of the theory and equations behind the strip-theory-based modeling approach is given in the HydroDyn User's Guide and Theory Manual [9]. Although FAST v8 now has the capability of modeling offshore fixed-bottom multimember substructures with flexible members, structural flexibility is not currently a feature for floating platforms.

FAST v8 is now able to simulate second-order wave kinematics for the strip-theory-based modeling approach and second-order incident-wave excitation (diffraction) forces for the potential-flow-based modeling approach [9]. The implementation of second-order hydrodynamic theory enables more accurate modeling of sea states and the associated wave loads on fixed-bottom and floating wind systems. The magnitude and frequency content of second-

2

order hydrodynamic loads can excite structural natural frequencies, leading to greater ultimate and fatigue loads. A circumstantial verification of these new second-order modeling capabilities was not part of the scope of this paper, but selected examples of simulation results that illustrate the second-order effects are given in the results section. Further information on the verification of the second-order modeling capabilities implemented in FAST v8 can be found in [10].

The new quasi-static mooring line module MAP was also part of this verification study. MAP replaces the original quasi-static mooring line model of FAST v7. In addition to quasi-static, single-segment mooring systems, MAP can also model multisegmented mooring lines [3]. Multisegemented mooring systems involving variable stiffness and mass properties and line-to-line interconnections have widespread, practical utility in realistic offshore anchoring designs. This new multisegment feature, however, is not part of the verification work covered within this paper.

III. Model Description

The model used to verify the new HydroDyn capabilities follows the definition of the OC4-DeepCwind floating semisubmersible wind turbine [4]. The turbine used for this model was the NREL 5-MW reference turbine [11]. The floating semisubmersible platform was based on the DeepCwind project [12]. Because FAST v8 offers three different approaches for calculating hydrodynamic loads (potential-flow theory only, potential-flow theory combined with viscous drag from Morison's equation, and strip-theory only), three different FAST v8 models were created. All three models described below used HydroDyn's new ballasting feature for modeling the water mass in the partially flooded platform columns [4]. The current implementation of the ballasting feature requires the user to hand-calculate the (4, 4), (5, 5), (4, 6), and (5, 6) entries of the 6 x 6 linear hydrostatic restoring matrix (*AddCLin* in the HydroDyn input file) to model the ballasting-induced restoring moments. A detailed description of these terms is given in Section 6.8.3 of the HydroDyn User's Guide [9].
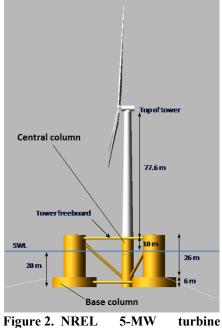
A. WAMIT-Only Model

From here on the potential-flow-only model is referred to as the WAMIT-only model. The approach used to calculate the first-order hydrodynamic loads for this model was the same as in FAST v7. Linear hydrostatic restoring, wave radiation, and diffraction forces were considered through a set of hydrodynamic coefficients that were calculated via WAMIT. In accordance with the OC4 model description [4], a quadratic drag matrix was added to the model to mimic viscous drag effects that otherwise would not be captured by the WAMIT-only approach.

Second-order difference-frequency potential-flow terms can be included in FAST v8 via a Newman approximation, which is based on first-order WAMIT coefficients, or by considering the full difference-frequency quadratic transfer functions (QTFs), derived from a second-order WAMIT solution. Second-order sum-frequency potential-flow terms can also be included via a full sum-frequency QTF, calculated from a second-order WAMIT solution [9]. The second-order, potential-flow-based simulation results shown in this paper were computed with the full sum- and difference-frequency QTFs.

Figure 2. NREL 5-MW turbine installed on the OC4 platform [4].

B. WAMIT+Morison Model

The hybrid model that combines the viscous-drag term from Morison's equation and the potential-flow theory approach will be referred to as the WAMIT+Morison model. In addition to the hydrodynamic load calculation features described for the WAMIT-only model, the WAMIT+Morison model calculates viscous drag forces for each member of the submerged platform geometry based on the local wave particle and structural velocities, rather than using an additional quadratic drag matrix (as used for the WAMIT-only model). The ability to model viscous drag at the member-level for a complicated multimember substructure like the OC4-DeepCwind semisubmersible was not available in FAST v7 (in FAST v7, only viscous drag on a central column could be modeled). This new HydroDyn feature is a valuable tool for augmenting a potential-flow based model with viscous-drag loads induced by flow

3

separation. For a substructure that consists of members with different diameters, the viscous drag component can play an important role, especially for members that are relatively small in diameter.

The platform geometry and the corresponding drag coefficients were defined based on the OC4 model description [4], and on the information given in the following section. Only first-order wave kinematics were considered in this paper for this model (even for the model with second-order WAMIT). This WAMIT+Morison model with second-order WAMIT enabled is distributed with FAST v8.09.00a-bjj as test 25 in the certification test (CertTest directory).

C. Morison-Only Model

In the Morison-only model, hydrodynamic loads are calculated solely from a strip-theory approach. Compared to the potential-flow based approach, strip-theory hydrodynamic loads may be preferable for substructures with members that are relatively small in diameter, compared to the typical wave length. A Morison-only model does not require an additional preprocessor like WAMIT. Platform geometry and all required hydrodynamic coefficients are directly specified by the user in the HydroDyn input file. Because the present version of HydroDyn does not calculate the change in buoyancy with platform displacement when using a Morison-only approach, the user must manually include the hydrostatic restoring matrix through the definition of a linear stiffness matrix in the HydroDyn input file. The calculation of the required coefficients is described in [9]. In addition to the drag coefficients and platform geometry, the Morison-only model requires the definition of added mass and dynamic-pressure coefficients for each member and joint. The selection of the appropriate hydrodynamic coefficients was based on the information provided in [4]. Several adjustments from the original OC4 model description [4] were introduced to the definition of added mass and drag coefficients for member joints in the heave direction. These adjustments were necessary because of the FAST v8-specific implementation of the hydrodynamic loads in the axial/heave direction. In [4], the base columns (Fig. 2) were considered as heave plates for the computation of drag forces in the axial direction. The axial drag coefficient of 4.8, as described in [4], was based on the assumption that the base column is a flat heave plate with an equal area on the top and bottom. Because FAST v8 considers the actual wetted surface of the members, and the top column is connected to another member, the top of the base column contributes a smaller surface area to the axial drag force calculation than the bottom. To create a FAST v8 model that behaves similar to the one described in [4], the axial drag coefficient was doubled to 9.6 and applied only to the bottom of the base column.

The added mass coefficients in the heave direction were defined as 1.0 at the bottom of the central column (Fig. 2) and the base columns. Based on the new implementation in HydroDyn, the relationship between the added-mass coefficient in the axial direction of each joint (C_{Ai}) and the zero-frequency limit added mass in the heave direction (calculated via WAMIT) for a structure with N joints (assuming negligible transverse added mass from the pontoons and braces), is as follows:

$$\sum_{i=1}^{N} \left[\frac{C_{Ai} \vec{V}_{ni} \vec{V}_{ni}^{\,T}}{\sqrt{\vec{V}_{ni}^{\,T} \vec{V}_{ni}}} \right]_{33} = \frac{A_{33}(0)}{\rho_w} \tag{1}$$

with the added-mass coefficients at the bottom of the base and central column being defined as 1.0, and $A_{33}(0)/\rho_w$ being calculated as 1.50E+04 m³ by WAMIT. The added mass coefficients for the top ends of the base columns can be calculated via Eq. (1). The weighted normal reference volume vector ($\vec{V}_{ni}$) is further specified in [9] and considers the size and orientation of all member endplates connected to joint i. This approach ensures that the nonwetted contact area between the two connecting members on top of the base columns is not considered for the added mass force computation. Based on Eq. (1) and the definition of the normal volume vector given in [9], this eventually led to a C_{Ai} value of 0.428 for the top of the base columns.

In addition to the added mass and drag forces, the FAST v8 implementation of the Morison-only approach also considered fluid-inertia forces on the member ends. Similar to the transverse fluid-inertia forces from Morison's equation, the computation of the inertial forces at member ends is described in [9] and includes contributions from the local dynamic pressure (Froude-Kriloff) and scattering (fluid acceleration). The implementation in HydroDyn makes use of the added-mass coefficient discussed in the previous paragraph and requires the definition of dynamic pressure coefficients on the top and bottom of each member. The dynamic pressure coefficients at the bottom of the base column and central column were set to 1.0, and the dynamic pressure coefficient at the top end of the base columns were set to 0.5. The OC4 model description [4] did not address the scattering term or discuss dynamic pressure coefficients, and these values were found to create a reasonable system response for regular wave load

4

cases when being compared to the corresponding WAMIT-only results. A detailed description of the hydrodynamic load calculation for the Morison-only modeling approach is given in the HydroDyn User's Manual [9].

Second-order wave kinematics for the strip-theory-based approach, including second-order sum-frequency and difference-frequency terms, can be enabled by the user. These terms are computed from analytical full difference- and sum-frequency QTFs [9] and are included in some of the load cases.

IV.   Load Cases

The load cases included in the verification work are based on the OC4 project [5]:

Table 1. Simulated Load Cases

Load Case	Description	Degrees of Freedom (DOFs)	Wind	Waves/Current
LC 1.2	Static Equilibrium	All	No air	Still water
LC 1.3a	Free decay, surge	Platform	No air	Still water
LC 1.3b	Free decay, heave	Platform	No air	Still water
LC 1.3c	Free decay, pitch	Platform	No air	Still water
LC 1.3d	Free decay, yaw	Platform	No air	Still water
LC 2.1	Regular waves	Platform, Tower	No air	Regular Airy, H = 6 m, T = 10 s
LC 2.2	Irregular waves	Platform, Tower	No air	Irregular Airy, H_s = 6 m, T_p = 10 s, JONSWAP
LC 2.3	Current only	Platform, Tower	No air	0.5-m/s surface current, $1/7^{th}$ power law decrease with depth
LC 2.4	Current and regular waves	Platform, Tower	No air	0.5-m/s surface current, $1/7^{th}$ power law decrease, regular Airy, H = 6 m, T = 10 s
LC 2.5	50-year extreme wave	Platform, Tower	No air	Irregular Airy, H_s = 15 m, T_p = 19.2 s, JONSWAP
LC 2.6	White noise waves	Platform, Tower	No air	White noise waves, PSD = 1 m²/Hz for 0.05 Hz–0.25 Hz
LC 3.1	Deterministic wind and waves	All	Steady, 8 m/s	Regular Airy, H = 6 m, T = 10 s
LC 3.2	Stochastic wind (at rated) and waves	All	Turbulent, 11.4-m/s mean	Irregular Airy, H_s = 6 m, T_p = 10 s, JONSWAP
LC 3.3	Stochastic wind (above rated) and waves	All	Turbulent, 18-m/s mean	Irregular Airy, H_s = 6 m, T_p = 10 s, JONSWAP
LC 3.4	Wind/wave/current	All	Steady, 8 m/s	0.5 m/s surface current, $1/7^{th}$ power law, regular Airy, H = 6 m, T = 10 s
LC 3.5	50-year extreme wind/wave	All	Turbulent, 47.5-m/s mean	Irregular Airy, H_s=15 m, T_s=19.2 s, JONSWAP
LC 3.6	Wind/wave misalignment	All	Steady, 8 m/s	Regular Airy, H = 6 m, T = 10 s, direction = 30°
LC 3.7	White noise waves with steady wind	All	Steady, 8 m/s	White noise waves, PSD = 1 m²/Hz for 0.05Hz–0.25 Hz

V.   Verification Results

Key observations made during our FAST v8 verification work are discussed in the following sections. As described in [5], the large magnitudes of aerodynamic loads tend to mask the discrepancies between different hydrodynamic modeling approaches. Because this verification work is focused on the new hydrodynamic capabilities of FAST v8, the following sections do not cover load cases with aerodynamic loading. Even though the wind load cases (LC 3.x) are not further discussed within this paper, they were simulated as part of our FAST v8 verification work. Because no major changes were introduced to FAST's aerodynamic modeling capabilities, no

significant differences were found in a direct comparison of the LC 3.x simulation results generated by FAST v7 and the FAST v8 WAMIT-only model.

A. WAMIT Only

The WAMIT-only simulation results generated with FAST v8 (and second-order terms disabled) were virtually identical to FAST v7. Because FAST v7 did not have the capability of modeling partially flooded multimember substructure geometries directly in HydroDyn, the mass and inertia of any water ballast had to be included in the corresponding lumped mass and inertia values of the platform structural model. The new ballasting feature implemented in FAST v8 now enables the user to specify partially or fully flooded substructure members. The FAST v8 simulation results generated with this new ballasting approach showed small differences, compared to the corresponding FAST v8 simulations that included the water ballast as part of the lumped platform mass and platform inertia.
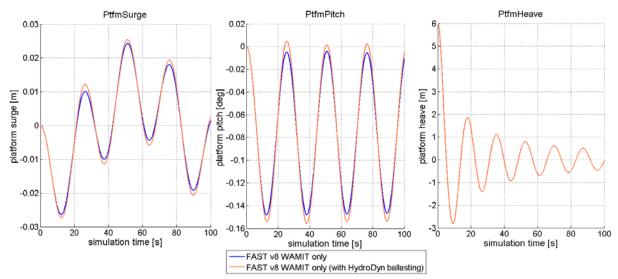

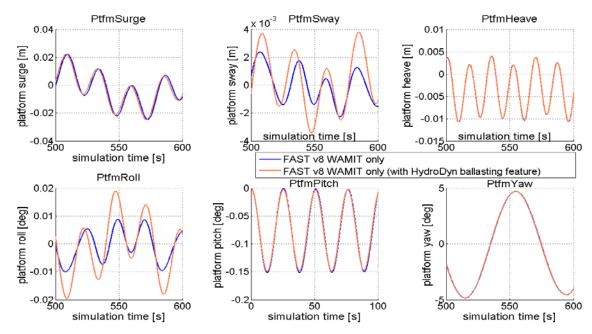**Figure 3. LC 1.3b simulation results (FAST v8 with and without HydroDyn ballasting).**

Figure 4. LC 1.3d simulation results (FAST v8 with and without HydroDyn ballasting).

6

The largest noteworthy differences between the FAST v8 simulations with and without HydroDyn ballasting occurred in the free-decay load cases: LC 1.3b and LC 1.3d. The system's pitch response with HydroDyn ballasting was slightly different in amplitude compared to a model incorporating the ballasting in the structural properties. The system's surge response, which was highly coupled to the pitch motion, also showed a small difference in amplitude. These differences can be explained as follows: the implementation of the ballasting feature in HydroDyn includes a small-angle assumption for the ballast-induced restoring moment in the pitch and roll degree of freedom (DOF) and it does not consider the nonlinear $\omega \times L$ inertia term (with ω being the angular velocity and L the angular momentum) of Euler's equation for rigid body rotations [13], which are both included when ballasting is part of FAST's structural model. Also, the rotational inertia of the ballast mass within the cross section of a member is not considered by the HydoDyn ballasting feature. These simplifications of the HydroDyn ballasting implementation explain the small differences in the coupled pitch and surge response, illustrated in Fig. 3 and Fig. 4.

The lack of significant differences between the WAMIT-only results from FAST v7 and FAST v8 also served as a verification of the new mooring line module, MAP, and the coupling approach introduced as part of the FAST v8 modularization framework.

B. WAMIT+Morison

In this section, the WAMIT+Morison results are compared against the corresponding WAMIT-only results, as well as against simulation results of other OC4 participants that use a combined Morison/potential-flow theory approach. The results for the free-decay load cases (LC 1.3a – LC 1.3d) agreed with the WAMIT-only results. Differences were visible in the coupled DOFs of the main free-decay motion (Fig. 5). This outcome was likely related to missing off-diagonal terms in the drag matrix that were used in the WAMIT-only model to mimic viscous-drag effects, and did not indicate a problem with the WAMIT+Morison solution [5].
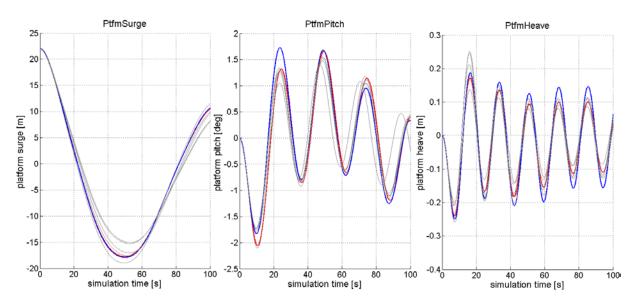

Figure 5. LC 1.3a simulation results (FAST v8 WAMIT+Morison, FAST v8 WAMIT only, WAMIT + Morison-only OC4 participants).

The regular wave response (LC 2.1) matched well with the corresponding WAMIT-only results. LC 2.3 and LC 2.4 were not simulated with the WAMIT-only model because hydrodynamic loading from current required the computation of member-level viscous-drag forces. In comparison to the other OC4 participants, the general system response predicted by FAST v8 for both the WAMIT+Morison and Morison-only models appeared to be reasonable (Fig. 6). The mean offset in surge due to the current induced viscous drag is adequately predicted by FAST v8. Enabling FAST's second-order wave potential-flow modeling capabilities for the WAMIT+Morison model in LC 2.4 increased the mean value of the platform surge signal as a result of second-order mean wave-drift loads (orange curve in Fig. 6). The results of several OC4 participants include corrections that induce higher order hydrodynamic effects (e.g. wave stretching or considering the instantaneous platform position). These higher order nonlinearities are not currently considered by FAST v8 and bring about an even larger increase of the mean platform surge.
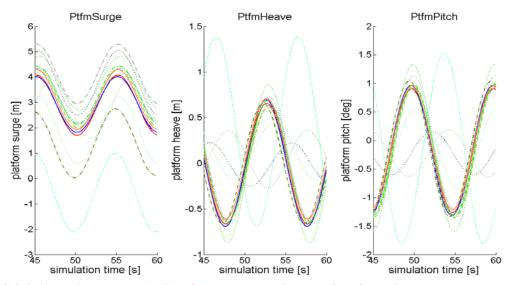
7

Figure 6. LC 2.4 simulation results (FAST v8 WAMIT+Morison, FAST v8 Morison-only, WAMIT+Morison OC4 participants, Morison-only OC4 participants, FAST v8 WAMIT+Morison with second-order theory).

The largest noticeable differences between FAST v8 and the other OC4 participants were found in the irregular wave load cases LC 2.2 and LC 2.5 when second-order potential-flow effects were not included. Simulation results of irregular wave simulations were analyzed in the frequency domain by comparing the corresponding power spectral density functions (PSDs). In LC 2.2, pitch, surge, and heave responses were under-predicted by FAST v8 at low frequencies when compared to WAMIT+Morison results of other OC4 participants (Fig. 7). A similar and even larger under-prediction of the low-frequency pitch, surge, and heave response was also evident in the Morison-only FAST v8 model when compared to Morison-only results of other OC4 participants and is further discussed within the next section. Although the underprediction of the surge motion by the FAST v8 WAMIT+Morison model was still visible in the simulation results for LC 2.5 (Fig. 8), the pitch and surge response were in better agreement with the other OC4 participants that use a combined Morison/potential-flow modeling approach. Enabling the second-order potential-flow terms in the WAMIT+Morison solution drastically increased the low-frequency response of the system in LC 2.2 and LC 2.5 (pink curves in Figs. 7 and 8) because of second-order slow- drift forces. This led to better agreement between FAST v8 and the other OC4 participants in the low-frequency range.
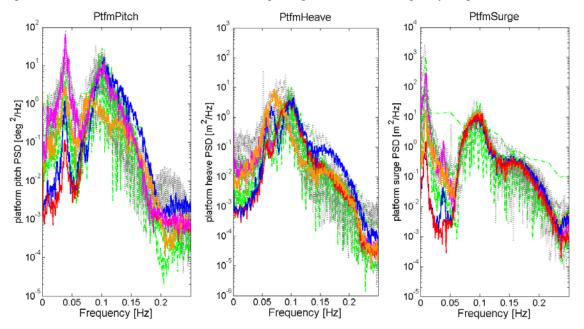

Figure 7. LC 2.2 simulation results (FAST v8 WAMIT+Morison, FAST v8 Morison-only, WAMIT+Morison OC4 participants, Morison-only OC4 participants, FAST v8 WAMIT+Morison with second-order wave theory, FAST v8 Morison-only with second-order wave theory).

8

C. Morison-Only

Compared to the WAMIT+Morison and WAMIT-only models, the Morison-only model uses a significantly different approach for the hydrodynamic load calculation. Therefore, differences in the simulation results were expected and a simple direct comparison against the WAMIT-only and WAMIT+Morison simulation results was of limited value for verification purposes.
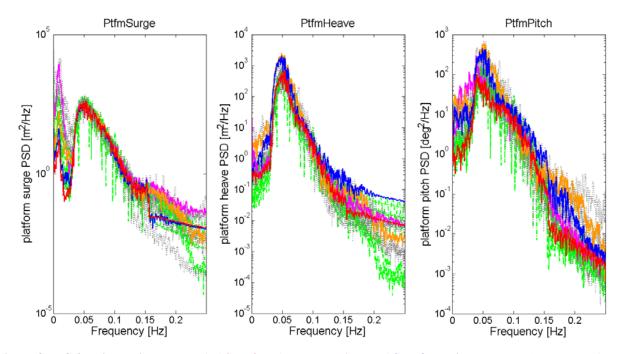

Figure 8. LC 2.5 simulation results (FAST v8 WAMIT+Morison, FAST v8 Morison-only, WAMIT+Morison OC4 participants, Morison-only OC4 participants, FAST v8 WAMIT+Morison with second-order wave theory, FAST v8 Morison-only with second-order wave theory).

For this reason, the FAST v8 Morison-only simulation results were mainly compared against the corresponding results of other OC4 participants that used a Morison-only modeling approach. The Morison-only FAST v8 results were similar to the other Morison-only OC4 participants for the free-decay (LC 1.3a – LC 1.3d) and regular wave (LC 2.1, LC 3.1, LC 2.4) load cases. The static-equilibrium position of the system with a constant surface current of 0.5 m/s (LC 2.3) was accurately predicted as well. FAST v8 also computed a reasonable system response for regular waves in combination with a constant surface current of 0.5 m/s, as illustrated in Fig. 6.

Differences between FAST v8 and the other Morison-only-based OC4 participants were found only in load cases with irregular waves (LC 2.2, LC 2.5). Between 0 Hz–0.05 Hz in the LC 2.2 PSD plot (Fig. 7), FAST v8 with first-order wave kinematics underpredicted the system response in surge, heave, and pitch. For LC 2.5, the FAST v8 Morison-only simulation results showed better agreement with the other Morison-only OC4 participants. As discussed for the WAMIT+Morison results, second-order hydrodynamics tended to increase the system response in the low-frequency band as a result of second-order slow-drift effects. This trend was also evident when comparing the blue (FAST v8 Morison-only) and the orange curves (FAST v8 Morison-only with second-order wave theory) in Figs. 7 and 8. The majority of the Morison-only OC4 participants did not consider second-order wave theory, but applied corrections by using the instantaneous position of the platform in the wave field or stretching the wave kinematics to the free surface, which induced higher-order hydrodynamic effects. As shown, the first-order FAST v8 simulation results underpredicted the system response for low frequencies, but the inclusion of second-order wave theory tended to capture much of the nonlinear effect. For LC 2.2 (Fig. 7), the first-order wave-excitation-induced peak around 0.1 Hz was shifted towards lower frequencies in the Morison-only solution with second-order wave kinematics (orange curve). This frequency shift was not evident for LC 2.5 (Fig. 8) and is being investigated further.

9

VI. Conclusions

With the latest release of FAST (v8), the hydrodynamic modeling capabilities of the software have been significantly extended. The user can now choose between the potential-flow (radiation/diffraction) based modeling approach, a strip-theory based modeling approach, and a hybrid approach (radiation/diffraction combined with the quadratic drag term from Morison's equation). The hybrid approach allows the user to augment a potential-flow-based model with additional viscous drag loads. The strip-theory-based approach may be preferable for substructures with members that are relatively small in diameter, compared to the typical wave length. Second-order hydrodynamic effects have also been implemented in HydroDyn, enabling the user to capture second-order hydrodynamic excitation forces, which can play an important role in the assessment of fatigue and ultimate load conditions.

Simulation results generated with FAST v8 were compared against the results of the previous FAST version (v7) and the results of other OC4 participants for a wide range of operating conditions. The load cases and model definition for this verification work was based on Phase II of the OC4 code comparison project. The new hydrodynamic modelling capabilities of FAST v8 were verified by comparing the simulation results against the results of OC4 participants with similar hydrodynamic modeling approaches.

Good agreement was found between the FAST v7 and the FAST v8 WAMIT-only simulation results, which verified the accuracy and reliability of the new quasi-static mooring line module MAP and the coupling approach that was introduced as part of the modular FAST v8 architecture.

The evaluation of the results generated with FAST v8 using a WAMIT+Morison and a Morison-only hydrodynamic modeling approach showed general agreement with the corresponding OC4 participants. The largest differences were found for load cases with irregular waves (LC 2.2 and LC 2.5) until second-order terms were included. The FAST v8 first-order results underpredicted the low-frequency system response compared to the majority of other OC4 participants. Enabling incident-wave excitation forces from second-order loads for the WAMIT+Morison potential-flow-based modeling approach significantly increased the low-frequency response of the system and improved the agreement between FAST v8 and the other OC4 participants. A similar trend was evident when enabling second-order wave kinematics for the FAST v8 Morison-only solution.

Acknowledgments

References

[1] Jonkman, J.; Buhl, M. (2005). FAST User's Guide. NREL/TP-500-38230. Golden, CO: National Renewable Energy Laboratory, 143 pp. Accessed November 3, 2014: http://www.nrel.gov/docs/fy06osti/38230.pdf.

[2] Jonkman, B.; Jonkman, J. (2014). ReadMe File for FAST v8.09.00a-bjj. Golden, CO: National Renewable Energy Laboratory. Accessed November 3, 2014: https://wind.nrel.gov/nwtc/docs/README_FAST8.pdf.

[3] Masciola, M. Instructional and Theory Guide to the Mooring Analysis Program. Golden, CO: National Renewable Energy Laboratory. Accessed November 3, 2014: http://wind.nrel.gov/designcodes/simulators/map/MAP_v0.87.06a-mdm.pdf.

[4] Robertson, A.; Jonkman, J.; Masciola, M.; Song, H.; Goupee, A.; Coulling, A.; Luan, C. (2014). Definition of the Semisubmersible Floating System for Phase II of OC4. NREL/TP-5000-60601. Golden, CO: National Renewable Energy Laboratory, 43 pp. Accessed November 3, 2014: http://www.nrel.gov/docs/fy14osti/60601.pdf.

[5] Robertson, A.; Jonkman, J.; Vorpahl, F.; Popko, W.; Qvist, J.; Froyd, L.; Chen, X.; Azcona, J.; Uzungoglu, E.; Guedes Soares, C.; Luan, C.; Yutong, H.; Pengcheng, F.; Yde, A.; Larsen, T.; Nichols, J.; Buils, R.; Lei, L.; Anders Nygard, T.; et al. (2014). Offshore Code Comparison Collaboration, Continuation within IEA Wind Task 30: Phase II Results Regarding a Floating Semisubmersible Wind System: Preprint. NREL/CP-5000-61154. Golden, CO: National Renewable Energy Laboratory, 17 pp. Accessed November 3, 2014: http://www.nrel.gov/docs/fy14osti/61154.pdf.

[6] Sprague, M.A.; Jonkman, J.M.; Jonkman, B.J. (2014). FAST Modular Wind Turbine CAE Tool: Nonmatching Spatial and Temporal Meshes: Preprint. NREL/CP-2C00-60742. Golden, CO: National Renewable Energy Laboratory, 26 pp. Accessed November 3, 2014: http://www.nrel.gov/docs/fy14osti/60742.pdf.

[7] Lee, C.H.; Newman, J.N. (2006). WAMIT User Manual (Version 6.4/6.4S). Massachusetts: WAMIT, Inc. Accessed November 3, 2014: http://www.wamit.com/manual6.htm.

[8] Jonkman, J.M. (2007). Dynamics Modeling and Loads Analysis of an Offshore Floating Wind Turbine. NREL/TP-500-41958. Golden, CO: National Renewable Energy Laboratory, 233 pp. Accessed November 3, 2014: http://www.nrel.gov/docs/fy08osti/41958.pdf.

[9] Jonkman J.; Robertson, A.; Hayman, G. (forthcoming). HydroDyn User's Guide and Theory Manual. Golden, CO: National Renewable Energy Laboratory.

[10] Duarte, T.; Sarmento, A. J. N. A.; Jonkman, J. (2014). Effects of Second-Order Hydrodynamic Forces on Floating Offshore Wind Turbines. NREL/CP-5000-60966. Golden, CO: National Renewable Energy Laboratory, 18 pp. Accessed November 3, 2014: http://www.nrel.gov/docs/fy14osti/60966.pdf.

[11] Jonkman, J.; Butterfield, S.; Musial, W.; Scott, G. (2009). Definition of a 5-MW Reference Wind Turbine for Offshore System Development. NREL/TP-500-38060. Golden, CO: National Renewable Energy Laboratory, 75 pp. Accessed November 3, 2014: http://www.nrel.gov/docs/fy09osti/38060.pdf.

[12] Masciola, M.; Robertson, A.; Jonkman, J.; Coulling, A.; Goupee, A. (2013). "Assessment of the Importance of Mooring Dynamics on the Global Response of the DeepCwind Floating Semisubmersible Offshore Wind Turbine." Proceedings of the Twenty-Third (2013) International Offshore and Polar Engineering Conference; June 30-July 5, 2013, Anchorage, Alaska. NREL/CP-5000-57869. Golden, CO: National Renewable Energy Laboratory; pp. 359-368.

[13] Ardema, M. (2005). Newton-Euler Dynamics. New York: Springer. pp. 20.